ACTA CHROMATOGRAPHICA, NO. 13, 2003

EFFECT OF PARTICLE-SIZE DISTRIBUTION AND PARTICLE POROSITY CHANGES ON MASS-TRANSFER KINETICS

K. Kaczmarski[1,*] and *J. Ch. Bellot*[2]

[1]Faculty of Chemistry, Rzeszów University of Technology, ul. W. Pola 2, 35-959 Rzeszów, Poland
[2]Centre de Bioingéniere Gilbert Durand, UMR-CNRS 5504, UMR-INRA 792, INSA, 135 av. de Rangueil, 31077 Toulouse, Cedex 4, France

ABSTRACT

Effective mass-transfer kinetics depend on particle-size distribution (PSD) and particle porosity (among other complex phenomena). The pore-diffusion flux can vary with adsorbate loading – if the amount of adsorbed species is sufficiently large it can lead to hindrance effects that substantially change particle porosity.

By use of batch kinetic adsorption experiments the general rate model was used to investigate the effect of PSD and variation of particle porosity on the pore-diffusivity coefficient, D_p. It was proved that neglecting these phenomena can lead to misinterpretation of experimental data. Modelling of HPLC profiles using PSD and conventional modelling with mean diameters was also examined and compared.

INTRODUCTION

The use of preparative liquid chromatography for separation and purification of pharmaceutically and biologically active compounds is increasing. Chromatographic separations usually involve complex mass-transfer mechanisms that strongly affect band profiles. To enable accurate prediction of these processes, therefore, mass-transport kinetics should be quantitatively described in addition to equilibrium thermodynamics. Indeed, a correct mathematical model of these kinetics is necessary for accurate optimization of separations for maximum productivity of the process.

When the mass transport kinetics are slow, the general rate model (GR) is the most accurate tool for prediction of band profiles. This model takes good account of all contributions to band broadening, i.e. axial

dispersion and external and internal mass-transfer resistance, and provides a reliable method for calculation of elution band profiles [1–5]. Most crucial for modelling of band profiles, except for thermodynamics, seems, however, to be intra-particle diffusion, which is usually the rate-limiting step [5–8]. Research into mass transfer resistance inside particles has therefore become an intriguing field in fundamental studies of separation processes.

Adsorption of proteins on contemporary adsorbents can be extremely high [9,10]. Hunter and Carta [9] reported adsorption of 280–290 mg bovine serum albumin (BSA) per millilitre of adsorbent (a polymeric anion exchanger BRX-Q). Chen et al. [10] measured adsorption of approximately 150 mg mL^{-1} BSA on DEAE Spherodex M. Such large amounts of adsorbed protein can substantially change the pore volume of adsorbent available for the species present and can considerably affect the mass flux inside particles. (Pore clogging by sintering or coking is well known in chemical reactor engineering [11,12].)

The effect of partial clogging of the pores by adsorbed species was envisaged by Liapis et al. [13], Hunter and Carta [9], and Chen et al. [10]. Gritti et al. [14] have recently demonstrated that during adsorption of butyl benzoate on a monolithic RPLC column the total porosity and, especially, the mesopore porosity is changing substantially, depending on the concentration of butyl benzoate in the liquid phase. In their next paper Piątkowski et al. [15] proved that for robust modelling of diffusion inside a monolithic column the GR model should be used. Indeed, this model can successfully predict chromatographic band profiles even when the mesopore volume changes because of adsorption of feed components on the pore surface of the adsorbent. Excellent agreement was obtained between experimental and calculated band profiles.

Variations of mesopore volume affect HPLC peaks and breakthrough curve profiles and also the shape of uptake curves obtained from stirred-batch adsorption experiments (see results and discussion section). These uptake curves are frequently used for evaluation of pore-diffusivity coefficients, D_p [9,10]. By using such an experimental method, Chen et al. [10] investigated pore diffusivity for BSA and γ-globulin in the anion exchanger DEAE Spherodex M and found that the D_p values obtained decrease markedly with increasing initial concentration of the species. It will be shown in this paper that this dependence can result from ignoring changes of adsorbent porosity during the adsorption process. Approxima-

tion of real particle-size distribution (PSD) by use of average diameter can, moreover, lead to misinterpretation of experimental data.

The first aim of the work discussed in this paper was to illustrate the effect of adsorbent pore clogging on uptake curves obtained from stirred-batch adsorption experimental data available in the literature. We would like to point out the role of obstruction by adsorbed molecules on the dependence of pore diffusivity on species concentration. The second aim was to investigate the effect of PSD on theoretical uptake curves from stirred-batch adsorption experiments and on HLPC peak profiles.

THEORY

Model of Differential Mass Balance for Stirred-Batch Adsorption

The differential mass balance for the species in the fluid phase can be expressed as:

$$\varepsilon_e \frac{\partial C}{\partial t} = -(1-\varepsilon_e)\frac{3}{R} \times \varepsilon_p D_p \left.\frac{\partial C_p}{\partial r}\right|_{r=R} \tag{1}$$

initial condition
for $t = 0$

$$C(0) = C_0 \tag{2}$$

The mass balance equation for a particle is:

$$\frac{\partial\left(\varepsilon_p(q)\, C_p\right)}{\partial t} + \frac{\partial q}{\partial t} = \frac{1}{r^2}\frac{\partial}{\partial r}\left(r^2 D_p\ \varepsilon_p(q)\frac{\partial C_p}{\partial r}\right) \tag{3}$$

initial condition
for $t = 0$

$$q(r,0) = 0 \tag{4}$$

$$C_p(r,0) = 0$$

boundary conditions
for $r = 0$

$$\frac{\partial C_p}{\partial r} = 0 \tag{5}$$

for $r = R$

$$C_p = C \tag{6}$$

In these equations C and C_p (mg mL^{-1}) are the concentrations of the solute outside the particle and in the stagnant liquid phase, respectively, q (mg mL^{-1}) is the concentration of adsorbed component, t is the time, r is the distance from the particle centre, R is the particle radius, ε_e is the external porosity, ε_p the internal or particle porosity, and D_p is the pore-diffusivity coefficient.

The model described by eqs (1–6) is compatible with that used by Chen et al. [10].

To consider PSD conditions, eq. (1) was modified to eq. (1a) as follows:

$$\varepsilon_e \frac{\partial C}{\partial t} = -\varepsilon_p D_p \sum_i \left(\frac{(1-\varepsilon_{ei}) \times 3}{R_i} \frac{\partial C_{pi}}{\partial r}\bigg|_{r=R} \right) \tag{1a}$$

where i denotes the ith fraction of particle-diameter distribution, and external porosity ε_{ei} is an hypothetical external porosity when only the ith fraction exists, calculated by use of the relationship:

$$\varepsilon_{ei} = 1 - (1-\varepsilon_e) \times \frac{V_i}{V_a} \tag{7}$$

where V_i is the volume of the ith fraction and V_a is the total volume of adsorbent. Equation (1a) was solved with eq. (3) for each particle diameter. Finally, the differential mass balance model was coupled with the Langmuir isotherm model:

$$q = \frac{q_m \times C_p}{K_d + C_p} \tag{8}$$

where q_m is the adsorption capacity and K_d the dissociation constant.

Numerical Solution of the Model

The model described above gives equations that were solved by use of the global orthogonal collocation method [16] with 20 collocation points. The set of discretized ordinary differential equations was solved by the Adams–Moulton method, implemented in the VODE procedure [17]. The relative and absolute errors of the numerical calculations were 1×10^{-6} and 1×10^{-8}, respectively.

Investigation of Particle-Size Distribution

The particle size of a packing is of utmost importance. Particles used in HPLC and, especially, in expanded bed chromatography can vary widely in size [18, 19]. This particle-size distribution can be handled in several different ways. The most popular definitions are [20]:

1. The arithmetic mean:

$$d_{10} = \frac{\sum_i n_i d_i}{N} \tag{9}$$

where $N = \sum_i n_i$, i is an index of the population, and d_i is the particle diameter of population i.

2. The volume mean:

$$d_{30} = \left(\frac{\sum_i n_i d_i^3}{N} \right)^{\frac{1}{3}} \tag{10}$$

3. The volume-surface mean:

$$d_{32} = \frac{\sum_i n_i d_i^3}{\sum_i n_i d_i^2} \tag{11}$$

4. The volume-moment mean:

$$d_{43} = \frac{\sum_i n_i d_i^4}{\sum_i n_i d_i^3} \tag{12}$$

The volume-moment mean (volume- or weight-moment mean) particle size is that most often reported in the chromatography literature, but not everybody abides by this convention [18].

In this work we have compared uptake curves calculated for the PSD presented in Figs 1b and 1d in Ref. [21] with profiles calculated for a mean particle diameter obtained from eqs (11) and (12). Because the PSD was read from the figures, the calculated mean diameter differs slightly

from that given by the authors of Ref. [21]. Because of the illustrative purpose of this work, however, we ignored this discrepancy.

The frequency distribution is given in Table I. The calculated values of the mean diameters (d_{10}, d_{30}, d_{32}, and d_{43}) are listed in Table II.

Table I

Frequency distribution for p-PE1 and Streamline DEAE calculated from data given in Figs 1b and 1d, Ref. [21]

Fig 1b		Fig 1d	
N_i/N (%)	d (μm)	N_i/N (%)	d (μm)
1.6	18	0.39	65
4.3	20	0.71	75
3.3	22	1.7	95
3.8	24	6.3	105
2.6	26	9.135	115
2.2	28	16.2	125
3.28	30	23	135
4.34	32	12	145
12.4	34	9.135	155
8.2	36	8.033	165
14.6	38	3.072	175
20.5	40	3.704	185
4.84	42	1.97	195
4.67	44	0.77	205
5	46	0.705	215
3.2	48	0.705	225
1.17	50	0.47	245
–	–	1	275
–	–	1	295

Table II

Calculated values of mean particle diameters

Adsorbent	d_{10} (μm)	d_{30} (μm)	d_{32} (μm)	d_{43} (μm)
p-PE1	35.9	37.3	38.6	39.6
Steamline DEAE	143.2	151.5	160.8	173.7

Investigation of the Hindered Diffusion Model

To investigate the role of pore clogging we used the experimental conditions of Chen et al. [10], presented in Tables III and IV. The volume-weighted mean particle size, d_{43}, of the adsorbent DEAE Spherodex M is 83 μm. The particle-size distribution was not given in Ref. [10]. The effective particle porosity ε_p was 0.616 and 0.440 for BSA and γ-globulin, respectively. Because the ratio of liquid phase to total volume of liquid and solid phase, ε_e, was not given, we estimated this value to obtain exact agreement between solution of the stirred-batch adsorption model and the batch kinetic experiments presented in Figs 2 and 3 in Ref. [10].

Table III

Values of model terms [10]

Isotherm coefficients		Approximation of ε_e			
q_m (mg mL^{-1})	K_d (mg mL^{-1})	BSA		γ-Globulin	
BSA		C_0 (mg mL^{-1})	ε_e	C_0 (mg mL^{-1})	ε_e
169.5	0.017	0.3	0.995	0.3	0.989
		0.7	0.995	0.5	0.9901
γ-Globulin		1.2	0.9946	1.0	0.9901
87.7	0.5	1.6	0.9947	1.3	0.99
		2.2	0.9919	1.8	0.9884

Table IV

Values of pore-diffusivity coefficients [10]

BSA		γ-Globulin	
C_0 (mg mL^{-1})	$D_p \times 10^{11}$ (m^2 s^{-1})	C_0 (mg mL^{-1})	$D_p \times 10^{12}$ (m^2 s^{-1})
0.3	6.88	0.3	7.60
0.7	6.57	0.5	6.79
1.2	5.96	1.0	5.90
1.6	5.67	1.3	5.09
2.2	5.10	1.8	4.65

RESULTS AND DISCUSSION

Effect of Particle-Pore Clogging on Effective Values of the Pore-Diffusivity Coefficient, D_p

To interpret their data Chen et al. [10] assumed a dominant role of pore diffusivity in mass transfer inside adsorbent particles. Fitting of experimental kinetic experiments with the pore diffusion model gave the desired value of D_p. The results obtained by Chen et al. [10] are depicted in Table IV. It is apparent that pore diffusivity decreases with increasing initial concentration C_0. Chen et al. [10] ignored the dependence of particle porosity on concentration ε_p. In this work we re-interpreted their results, assuming that particle porosity is a linear function of the amount of adsorbed species, q:

$$\varepsilon_p(q) = \varepsilon_p^o - p \times q \tag{13}$$

The values of p and the pore-diffusivity coefficient, D_p, were estimated to obtain the best agreement between theoretical uptake curves and experimental curves for $C_0 = 0.3$ and $C_0 = 2.2$ in the BSA experiments and $C_0 = 0.3$ and $C_0 = 1.8$ in the γ-globulin experiments. In the BSA experiments the best fitting terms were $D_p = 1.22 \times 10^{-10}$ m^2 s^{-1} and $p = 0.002363$ mL mg^{-1}; in the γ-globulin experiments $D_p = 9.08 \times 10^{-12}$ m^2 s^{-1} and $p = 0.005$ mL mg^{-1}. These values were used to calculate uptake curves for other initial concentrations.

Experimental and theoretically simulated data are compared in Figs 1 and 2. Agreement between experimental and theoretical profiles is relatively good. It should be emphasized that this good agreement was obtained for a constant value of pore diffusivity. The estimated value of BSA pore diffusivity is surprisingly high, 1.7 times greater than for the bulk phase (i.e. 6.95×10^{-11} m^2 s^{-1} [22]). Chen et al. [10] obtained similar results. To avoid this inconvenience they assumed that surface diffusion plays a significant role in intraparticle mass transfer.

The other reason for such large values of D_p might be a consequence of ignoring PSD – see below. It is also possible that overestimation of the diffusivity is connected with incorrect estimation of effective particle radius – a diffusion path available for the particle. It has already been pointed out that the effective particle porosity, ε_p, was 0.616 and 0.440 for BSA and γ-globulin, respectively [10]. Taking this into account, and remembering that γ-globulin is three times larger than BSA, it seems that large fractions of DEAE particle pores are so narrow they are hardly

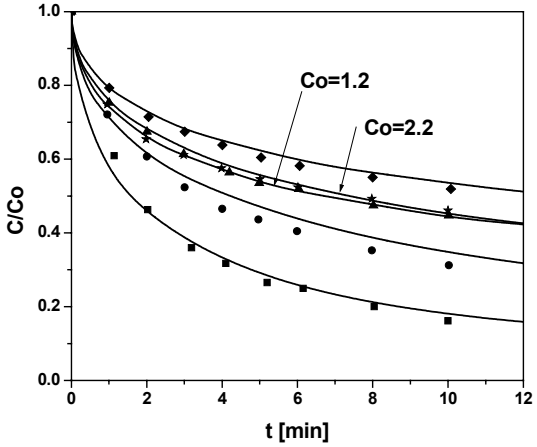

Fig. 1

Experimental (symbols) and simulated (solid lines) uptake curves depicting the effect of changes of particle porosity on the amount of adsorbed BSA. ■ $C_0 = 0.3$, ● $C_0 = 0.7$, ▲ $C_0 = 1.2$, ♦ $C_0 = 1.6$, ★ $C_0 = 2.2$ mg mL^{-1}. $D_p = 1.22 \times 10^{-10}$ m^2 s^{-1} and $p = 0.002363$ mL mg^{-1}.

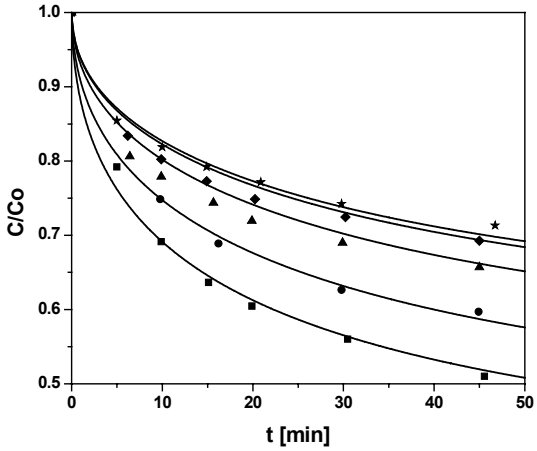

Fig. 2

Experimental (symbols) and simulated (solid lines) uptake curves depicting the effect of changes of particle porosity on the amount of adsorbed γ-globulin. ■ $C_0 = 0.3$, ● $C_0 = 0.7$, ▲ $C_0 = 1.2$, ♦ $C_0 = 1.6$, ★ $C_0 = 2.2$ mg mL^{-1}. $D_p = 9.08 \times 10^{-12}$ m^2 s^{-1} and $p = 0.005$ mL mg^{-1}.

accessible by BSA. Assuming BSA can completely block pores, it can be concluded that the apparent diffusion distance inside the adsorbent is smaller than the particle radius. If this is true, real pore diffusivity is smaller than that evaluated by Chen et al. [10] and by us.

Effect of Particle-Size Distribution on Uptake-Curve Profiles

In this section the effect of particle-size distribution on uptake-curve profiles is investigated. This and the next section are only illustrative in character; we did not intend further and more precise interpretation of the data of Chen et al. [10], because they did not report the particle-size distribution of the adsorbent used.

To illustrate the discrepancy between the uptake curves calculated for PSD and mean diameters an ε_e value of 0.995 was assumed. The calculations were performed assuming a constant value of particle porosity $\varepsilon_p = 0.616$ and $D_p = 1.22 \times 10^{-10}$ cm^2 s^{-1}. The Langmuir isotherm terms were $q_m = 169.5$ mg mL^{-1} and $K_d = 0.017$ mg mL^{-1}. Plots of simulated uptake curves calculated for the particle-size distribution presented in Table I (symbols) and average diameters d_{32} and d_{43} given in Table II (solid lines) are compared in Figs 3 and 4. For small particle diameters the differences

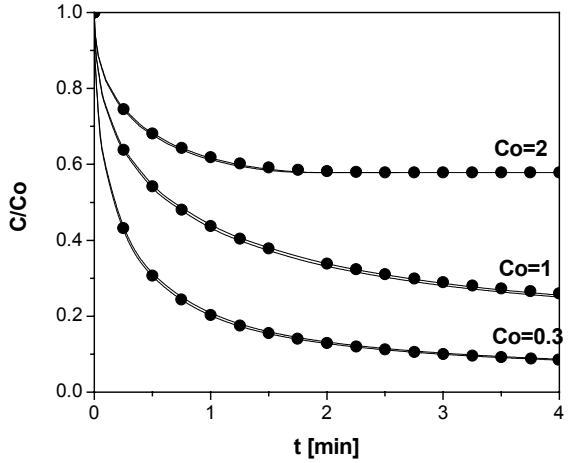

Fig. 3

Simulated uptake curves for $d_{32} = 38.6$ μm and $d_{43} = 39.6$ μm – lower and upper of double solid lines. Symbols denote simulated uptake curves calculated for particle-size distribution.

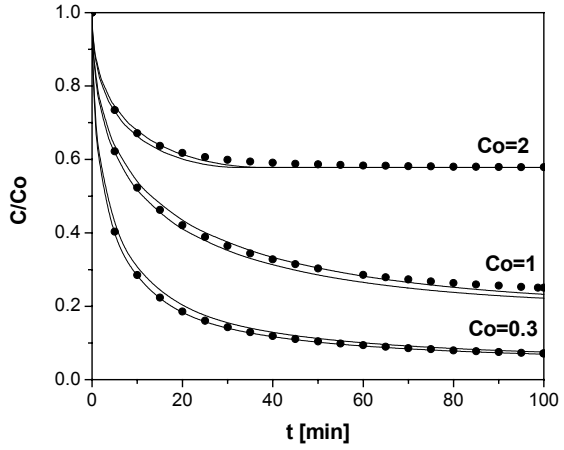

Fig. 4

Simulated uptake curves for d_{32} = 160.7 μm and d_{43} = 173.7 μm – lower and upper of double solid lines. Symbols denote simulated uptake curves calculated for particle-size distribution.

between PSD curves and simulations obtained for d_{32} and d_{43} are negligible (Fig. 3). For the large particle diameters frequently used in expanded-bed adsorption or other types of preparative chromatography, however, these differences are substantial (Fig. 4). From Fig. 4 it follows that for small concentrations the d_{32} curve is in best agreement with the PSD uptake curve. For higher concentrations and at the beginning of the experiment, however, the PSD curve coincides well with the d_{32} solid line but afterwards (for $C_0 = 2$ g L^{-1}), rises above the d_{32} and, next, the d_{43} curves; then, if the time is large enough, all the curves come back together.

From the relationship between PSD d_{32} and d_{43} curves it also follows that the apparent pore diffusivity value estimated from PSD uptake curves, for constant average particle size, can decrease with decreasing initial concentration, C_0. Assuming that the average particle diameter is d_{32} and that the points presented in Fig. 4 obtained for PSD are experimental data the best values of pore diffusivity evaluated are: for $C_0 = 0.3$, $D_p = 1.19 \times 10^{-10}$; for $C_0 = 1$, $D_p = 1.07 \times 10^{-10}$; for $C_0 = 2$, $D_p = 1.05 \times 10^{-10}$. Assuming, on the other hand, the average particle diameter is d_{43} the results obtained are: for $C_0 = 0.3$, $D_p = 1.40 \times 10^{-10}$; for $C_0 = 1$, $D_p = 1.24 \times 10^{-10}$; for $C_0 = 2$, $D_p = 1.22 \times 10^{-10}$.

From Fig. 5 is also follows that it might be impossible to obtain a perfect approximation of the uptake curves for PSD from the uptake curve calculated for average particle diameter.

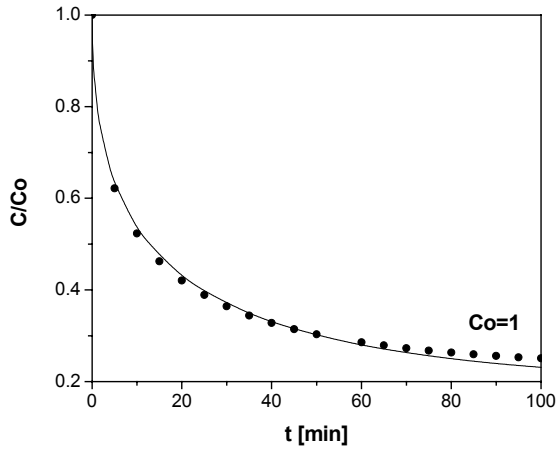

Fig. 5

The best approximation of the PSD uptake curve by use of the d_{43} curve.

Effect of Particle-Size Distribution on HPLC Peak Profiles

To investigate band profiles under HPLC conditions the data assumed were: column height $H = 0.1$ m, pore diffusivity $D_p = 3.7 \times 10^{-11}$ m^2 s^{-1}, external porosity $\varepsilon_e = 0.37$, particle porosity $\varepsilon_p = 0.5$, dispersion coefficient $D_L = 3.3 \times 10^{-9}$ m^2 s^{-1}, external mass transfer coefficient $k_{ext} = 4.5 \times 10^{-4}$ m s^{-1}, inlet concentration, $C_0 = 0.5$ mg mL^{-1}, injection time $t_j = 30$ s, superficial velocity $u = 1.33 \times 10^{-3}$ m s^{-1}. Calculations were performed for the linear, Langmuir, and anti-Langmuir isotherms.

$$q = \frac{a \times C}{1 + b \times C} \tag{14}$$

The value of a was always 15, and b was 0, 0.05, or –0.05 for linear, Langmuir or anti-Langmuir isotherms, respectively. The average frequency distribution was approximated using data from a plot of accumulated volume against particle diameter (presented in Fig. 4.3 of Ref. [18]) and is given in Table V. The volume-moment mean particle diameter d_{43} for the frequency distribution obtained is 5.13 μm. The simulations were performed with the general GR model for chromatography columns.

Table V

The average frequency used for simulation of HPLC peak profiles. V_i is the volume of fraction i and V is the total volume of particles

d (μm)	V_i/V (%)	d (μm)	V_i/V (%)
2.75	0	5.45	0.114
3.05	0.0012	5.75	0.093
3.35	0.0057	6.05	0.071
3.65	0.0262	6.35	0.05
3.95	0.0639	6.65	0.032
4.25	0.1087	6.95	0.019
4.55	0.131	7.25	0.01
4.85	0.138	7.55	0.004
5.15	0.132	7.85	0.0007

Equation (1a) was replaced by eq. (1b):

$$\varepsilon_e \frac{\partial C}{\partial t} + u\frac{\partial C}{\partial x} = \varepsilon_e D_L \frac{\partial^2 C}{\partial x^2} - \sum_i \left(\frac{(1 - \varepsilon_{ei}) \times 3k_{ext}(C - C_{pi}(r = R_i))}{R_i} \right) \quad (1b)$$

and coupled with the well known Danckwerts boundary conditions.

Equation (6) was replaced by eq. (6a):

$$D_p \varepsilon_p \frac{\partial C}{\partial r} = k_{ext}(C - C_{pi}(r = R_i)) \quad (6a)$$

for each particle-diameter fraction.

The GR model was solved using the orthogonal collocation on finite element method [4,5,16]. Results from comparison of peak profiles calculated for PSD and d_{43} mean diameter are presented in Fig. 6. Perfect agreement between band profiles was obtained in each simulation.

CONCLUSIONS

In this work it was proved that ignoring changes of particle porosity or particle-size distribution during interpretation of chromatographic data can lead to the conclusion that pore diffusivity depends on species concentration whereas in reality it can be constant. The error in the prediction of uptake curves or peak profiles when PSD is approximated by mean particle diameter decreases when particle diameter is reduced, and for the adsorbent diameters used in HPLC is negligible small. For particle sizes

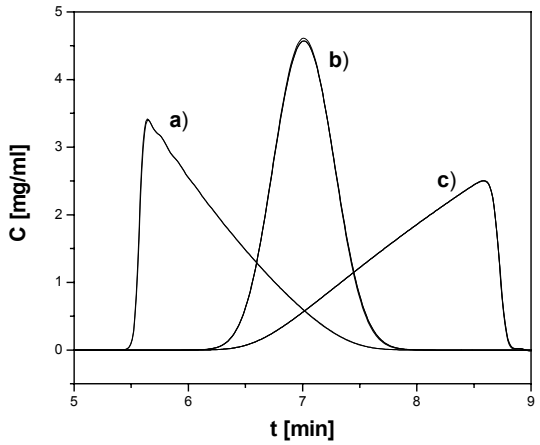

Fig. 6

Comparison of peak profiles calculated for PSD and d_{43} mean diameter: (a) Langmuir isotherm, (b) linear isotherm, (c) anti-Langmuir isotherm.

typically used in EBA, however, neglecting the PSD lead to misinterpretation of experimental data.

The concentration profiles calculated for PSD are located between curves calculated for volume-surface mean diameter d_{32} and volume-moment mean diameter d_{43}; for higher concentrations, however, profiles are better approximated by d_{43} mean.

In this paper the effect of pore clogging and PSD on uptake-curve profiles was studied separately. The next publication will report more precise analysis in which we couple these two approaches to obtain (we hope) better fitting of the experimental data and better approximation of the pore particle diffusivity.

ACKNOWLEDGEMENTS

This work was supported by Grant 4 T09C 006 23 of the Polish State Committee For Scientific Research.

REFERENCES

[1] D.M. Ruthven, Principles of Adsorption and Adsorption Process, Wiley, New York, NY, 1984

[2] M. Suzuki, Adsorption Engineering, Elsevier, Amsterdam, The Netherlands, 1990

[3] A.J. Berninger, R.D. Whitley, X. Zhang, and N.-H.L. Wang, Comput. Chem. Eng., **15**, 749 (1991)

[4] G. Guiochon, S. Golshan – Shirazi, and A.M. Katti, Fundamentals of Preparative and Nonlinear Chromatography, Academic Press, Boston, MA, 1994

[5] K. Kaczmarski, D. Antos, H. Sajonz, P. Sajonz, and G. Guiochon, J. Chromatogr. A, **925**, 1 (2001)

[6] G.L. Skidmore, B.J. Horstmann, and H.A. Chase, J. Chromatogr., **498**, 113 (1990)

[7] B.J. Horstmann and H.A. Chase, Chem. Eng. Res. Des., **67**, 243 (1989)

[8] A. Cavazzini, K. Kaczmarski, P. Szabelski, D. Zhou, X. Liu, and G. Guiochon, Anal. Chem., **73**, 5704 (2001)

[9] A.K. Hunter and G. Carta, J. Chromatogr. A, **897**, 81 (2000)

[10] W.-D. Chen, X.-Y. Dong, and Y. Sun, J. Chromatogr. A, **962**, 29 (2002)

[11] R. Hughes, Deactivation of Catalysts, Academic Press, New York, 1984

[12] H.S. Fogler, Elements of Chemical Reaction Engineering, Prentice Hall, Englewood Cliffs, New Jersey, 1999

[13] I.A. Liapis, J.J. Meyers, and O.K. Crosser, J. Chromatogr. A, **865**, 13 (1999)

[14] F. Gritti, W. Piątkowski, and G. Guiochon, J. Chromatogr. A, **983**, 51 (2003)

[15] W. Piątkowski, F. Gritti, K. Kaczmarski, and G. Guiochon, J. Chromatogr. A, in press

[16] V.J. Villadsen and M.L. Michelsen, Solution of Differential Equation Model by Polynomial Approximation, Prentice Hall, Englewood Cliffs, New Jersey, 1978

[17] P.N. Brown, A.C. Hindmarsh, and G.D. Byrne, Variable Coefficient Ordinary Differential Equation Solver, procedure available on http://www.netlib.org

[18] U.D. Neue, HPLC Columns. Theory, Technology, and Practice, Wiley–VCH, 1997
[19] J. Thommes, Fluidized Bed Adsorption as a Primary Recovery Step in Protein Purification, Advances in Biochemical Engineering, Biotechnology, Vol. 58, Springer, 1997
[20] H.G. Brittain, Pharm. Technol., **25**, 96 (2001)
[21] I. Theodossiou, H. D. Elsner, O.R.T. Thomas, and T.J. Hobley, J. Chromatogr. A, **964**, 77 (2002)
[22] M.T. Tyn and T.W. Gusek, Biotechnol. Bioeng., **35**, 327 (1990)